Supporting Information for manuscript

Pyrolytic cavitation, selective adsorption and molecular recognition of a porous Eu(III) MOF

Wei-Ming Liao, Hua-Tian Shi, Xu-Hua Shi and Ye-Gao Yin*

Department of Chemistry, Shantou University, Guangdong 515063, P. R. China.

E-mail: ygyin@stu.edu.cn, 11wmliao@gmail.com

Materials and Instruments

All reagents and solvents were purchased from commercial sources and used without further purification. Thermogravimetric analyses (TGA) were carried out on a Q50 TGA (TA) thermal analysis equipment under a nitrogen flow of (40 mL/min^{-1}) with a typical heating rate of 10℃/min^{-1}. Infrared spectra (KBr pellet) were recorded on a Nicolet Avatar 360 spectrophotometer in the range of 4000-400 cm^{-1}. Powder X-ray diffraction (PXRD) patterns of the samples were measured on a Bruker D8 Advance diffractometer (Cu Kα, λ = 1.5418Å) at room temperature. Gas adsorption isotherms of N_2, CO_2, H_2 and CH_4 were measured on the Micrometrics ASAP 2020 Surface Area and Porosity Analyzer. Elemental analyses of C, H, and N were determined with the instrument Elementar Vario EL III CHNS analyzer. UV-vis spectra of solvents were measured

with a Lambda 950 Spectrometer. Luminescence spectra were recorded on an Edinburgh Instruments FLS920 spectrofluorometer.

Experimental Section

Synthesis of $[(CH_3)_2NH_2]^+@[Eu_2L_3(HCOO)]^-$ (1)

A mixture of Eu_2O_3 (0.0352 g, 0.1 mmol), H_2**L** (0.0996 g, 0.6 mmol), DMF (2 mL), methanol (2 mL) and H_2O (2 mL) was sealed in a Pyrex tube and heated in an oven at 160℃ for 72 hours and then cooled slowly down to ambient at a rate of 5℃/h. Finally, colorless block-like crystals of **1** in yield of 75% were collected by filtration followed by washing with 3 portions of ethanol and drying. Elemental analysis (found/calcd: C% 36.43/36.51, H% 2.30/2.37, N% 1.62/1.58).

Synthesis of $[(CH_3)_2NH_2]^+@[Gd_2L_3(HCOO)]^-$ (2)

A mixture of Gd_2O_3 (0.0362 g, 0.1 mmol), H_2**L** (0.0996 g, 0.6 mmol), DMF (2 mL), methanol (2 mL) and H_2O (2 mL) in a Pyrex tube was heated in an oven at 160℃ for 72 hours and then cooled slowly down to room temperature at a rate of 5℃/h. The colorless block-like crystals of **2** (yield: 71%) were collected by filtration followed by washing with ethanol for 3 times and drying. Elemental analysis (found/calcd: C% 36.12/36.08, H% 2.31/2.34, N% 1.58/1.56).

Synthesis of $[(CH_3)_2NH_2]^+@[Sm_2L_3(HCOO)]^-$ (3)

The complex was prepared similarly to **1** and **2**, but using Sm_2O_3 in the place of Eu_2O_3 and Gd_2O_3 and isolated in yield of 64%. Elemental

analysis (found/calcd: C% 36.42/36.58, H% 2.42/2.37, N% 1.59/1.58).

CCDC reference numbers: 981208 for **2** and 981209 for **3**.

Pyrolysis of $[(CH_3)_2NH_2]$@$[Eu_2L_3(HCOO)]$

The TGA curve of **1** (Fig. S1) shows the desertion temperatures of $(CH_3)_2NH_2^+$ and $HCOO^-$ in the range of 280-350℃ and thus we ran the pyrolysis at 350°C. Powder of **1** was heated in a tube furnace (Hangzhou, SKC-5-12) for an hour under a nitrogen flow, and then **1-pyr** was attained after cooling down to room temperature. The PXRD spectrum of **1-pyr** (Fig. S3) confirms its crystallinity and microanalysis proves its composition as $[Eu_2L_3]$ (ratio sum of $[(CH_3)_2NH_2]^+$ and $[HCOO]^-$: found 10.45%, calcd 10.27%). Besides, its FT-IR spectrum (Fig. S2) shows no absorption of $[(CH_3)_2NH_2]^+$in the range of 2400 - 3200 cm^{-1}.

Crystal Structure Determination

Suitable crystals of complexes were mounted with glue at the end of a glass fiber. Data collection was performed on an Agilent Technologies Gemini A System (Cu Kα, λ = 1.54178 Å) at room temperature (293 K). The data were processed using software *CrysAlisPro.1*. The structure was solved by direct methods and refined by full-matrix least-squares refinements based on F^2. Anisotropic thermal parameters were applied to all non-hydrogen atoms. The H atoms were generated geometrically. The crystallographic calculations were performed using *SHELXL-97*[S1] programs. The void volume of lattice with $(CH_3)_2NH_2^+$ and $HCOO^-$

removed) was calculated using the program *PLATON*[S2]. Crystal data and structure refinements are summarized in Table S1.

Table S1 Crystal data and structure refinements for **1**-**3**.

Complexes	1	2	3
Chemical formula	$C_{27}H_{21}Eu_2NO_{14}$	$C_{27}H_{21}Gd_2NO_{14}$	$C_{27}H_{21}Sm_2NO_{14}$
Formula weight	887.39	897.95	884.17
crystal system	Triclinic	Triclinic	Triclinic
space group	*P-1*	*P-1*	*P-1*
a (Å)	8.38836(17)	8.3576(2)	8.3911(2)
b (Å)	10.5219(4)	10.5283(4)	10.5518(3)
c (Å)	17.3863(7)	17.4675(6)	17.4632(5)
α (deg)	99.169(4)	98.741(3)	98.993(3)
β (deg)	97.140(3)	97.008(3)	97.112(2)
γ (deg)	100.332(3)	100.523(3)	100.424(3)
V (Å^3)	1471.79(9)	1475.75(9)	1483.48(7)
Z	2	2	2
D_{Calcd}(g cm^{-3})	2.002	2.021	1.979
μ (mm^{-1})	4.294	4.526	3.990
Ref. collected	12827	11570	13786
Independent ref.	5982	5189	5219
R_{int}	0.0351	0.0348	0.0259
Goodness of fit	1.038	1.008	1.054
$R1^a$ [$I > 2\sigma(I)$]	0.0312	0.0262	0.0206
wR_2^b [$I > 2\sigma(I)$]	0.0716	0.0523	0.0428
$R1^a$ [all refl.]	0.0395	0.0325	0.0270
wR_2^b [all refl.]	0.0772	0.0558	0.0448

[a] $R_1=\sum(||F_0|- |F_c||)/\sum|F_0|$; [b] $wR_2=[\sum w(F_0^2- F_c^2)^2/\sum w(F_0^2)^2]^{1/2}$

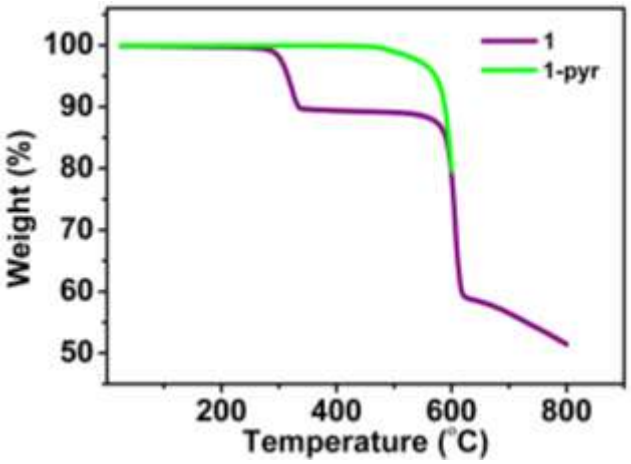

Fig. S1 TGA curves for **1** (black) and **1-pyr** (red).

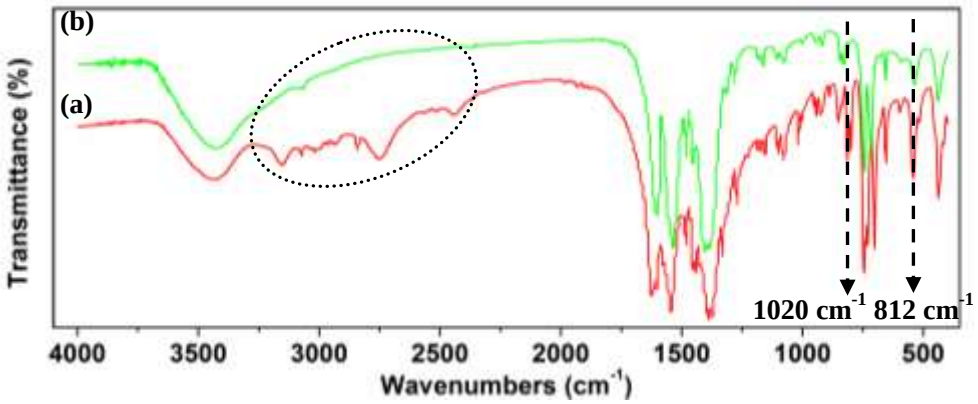

Fig. S2 Infrared spectra for **1** (a) and **1-pyr** (b).

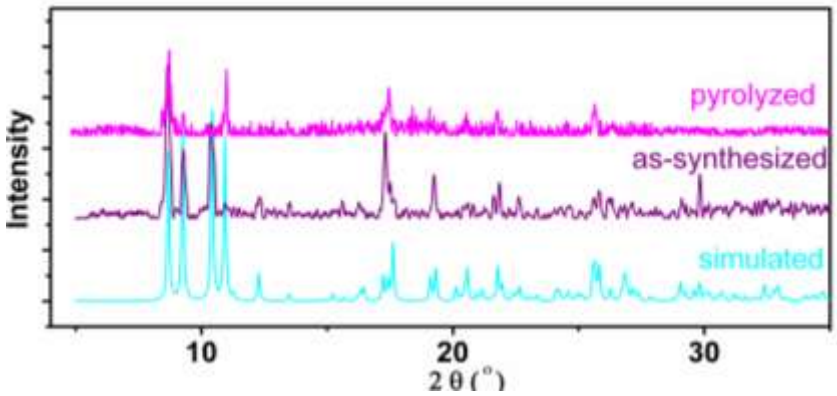

Fig. S3 The simulated and measured PXRD spectra for **1** (below) and **1-pyr** (middle) and that for **1-pyr** (upper).

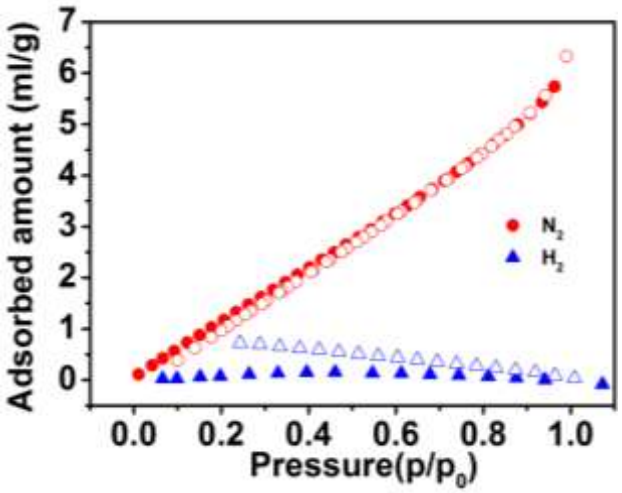

Fig. S4 N_2 and H_2 adsorption and desorption isotherms for **1** at 77K.

Fitting of Adsorption Isotherms

To have an insight into the nature of selective adsorption of **1-pyr**, we fit the CO_2 and N_2 adsorption isotherms by two models: i) just fit linear for the initial slopes (**Fig. S5**) and ii) single-site Langmuir (SSL) model. The model equation is:

$$q = \frac{q_{sat} bp}{1 + bp}$$

where q is the adsorption quantity, q_{sat} is the saturate adsorption quantity, b is the coefficients of Langmuir equation.

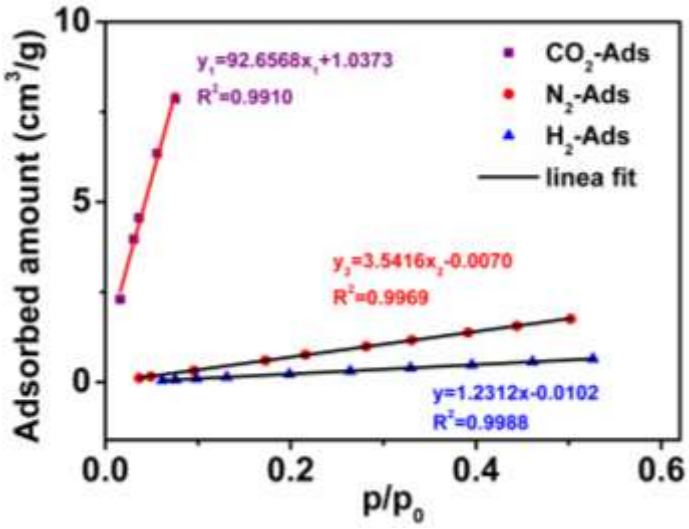

(a)

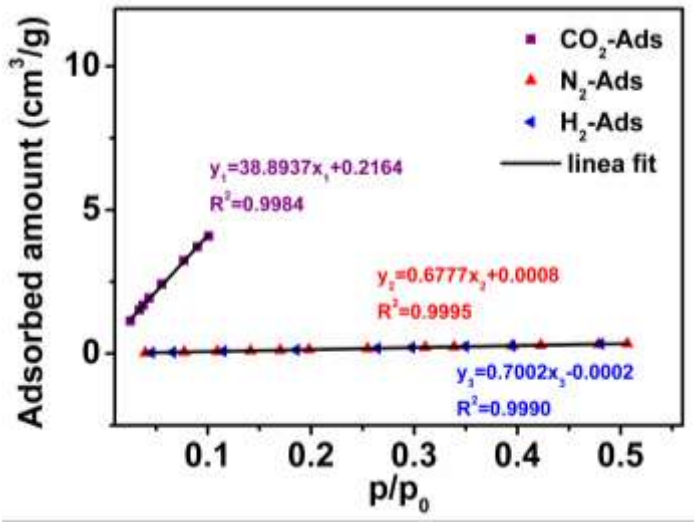

(b)

Fig. S5 The initial slopes for CO_2, N_2 and H_2 isotherms of **1-pyr** at 273 K (a) and 298 K (b).

Table S2 Gas adsorption performance of similar MOFs constructed from meta-benzenedicarboxylate units.

MOFs	Selectivity[a]	Selectivity[b]	S_{BET}[c](m^2/g^{-1})	CO_2 [d](wt%)	Reference
1-pyr	*57.4*	*72.5*	*124*	*3.6*	*this work*
HNUST-1	39.8(273K)	NA	1400	30.7	S3
MOF-177	17.73	NA	4690	26.59	S4
Cu-TDPAT	16	79	1938	6.2	S5
NOTT-122a	14.3	NA	3286	20.4	S6
MOF-74-Mg	12	NA	1495	35.2	S7
MMPF	NA	123(273K)	1205	13.2	S8
PCN-306	NA	40	1927	13.8	S9
PCN-61	NA	15	3350	NA	S10

NA, not available. [a] Selectivity calculated from the initial slopes of the isotherms at 298 K and 1 atm. [b] CO_2/N_2 (15 : 85) selectivity at 1 atm and 298 K calculated from Ideal Adsorbed Solution Theory (IAST). [c] Brunauer–Emmett–Teller (BET) surface area. [d] CO_2 uptake capacity at 298 K and 1 atm.

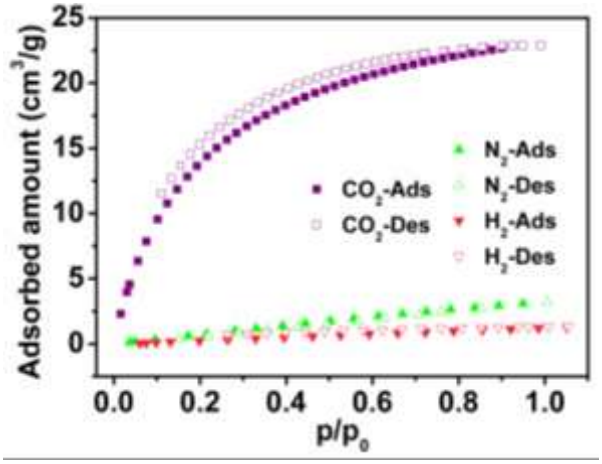

Fig. S6 Adsorption and desorption isotherms of **1-pyr** on CO_2, N_2 and H_2 at 273K.

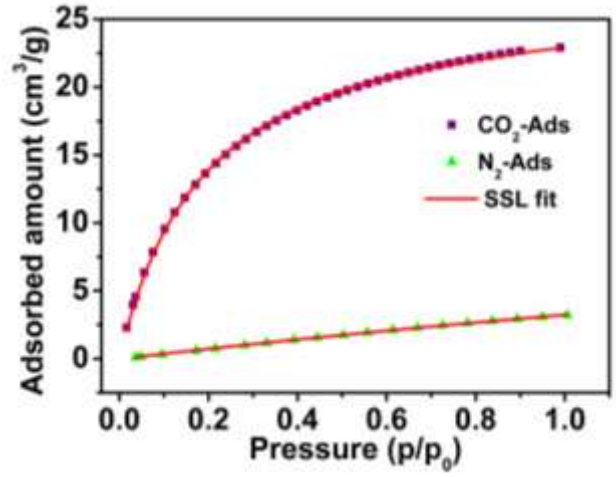

(a)

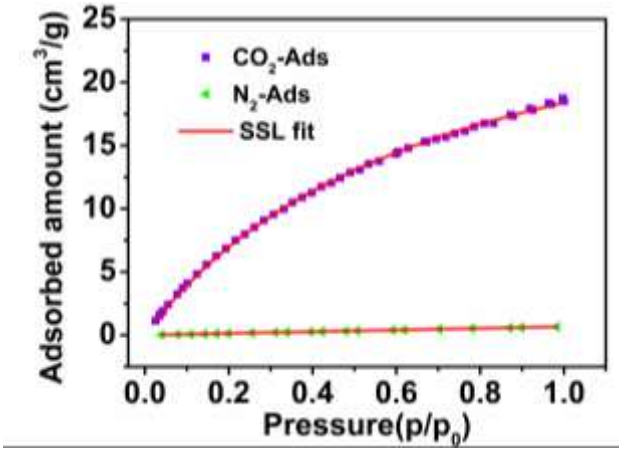

(b)

Fig. S7 The SSL fitting for the CO_2 and N_2 adsorption isotherms of **1-pyr** at 273K (a) and 298K (b).

Table S3 Single site Langmuir fitting parameters for CO_2 and N_2 adsorption at 273K and 298K.

CO_2	273K	298K
q_{sat}	27.352	31.188
b	5.172	1.438
R^2	0.99960	0.99953
Equation	y=27.352*5.172x/(1+5.172x)	y=31.188*1.438x/(1+1.438x)

N_2	273K	298K
q_{sat}	22.414	16.950
b	0.169	0.040
R^2	0.99957	0.99988
Equation	y=22.414*0.169x/(1+0.169x)	y=16.950*0.040x/(1+0.040x)

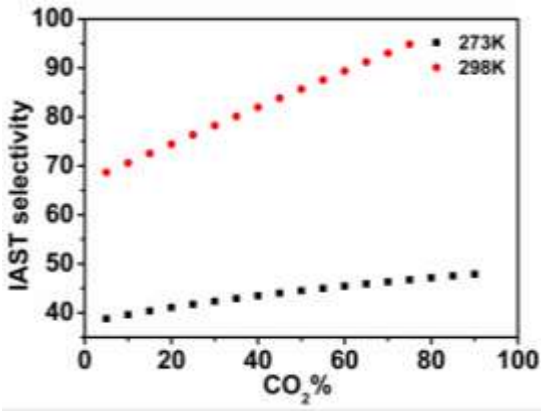

Fig. S8 The predicted IAST selectivity of CO_2/N_2 at 273 K and 298 K for **1-pyr**, showing the relation between IAST selectivity and various percentage of CO_2 in the two component mixture.

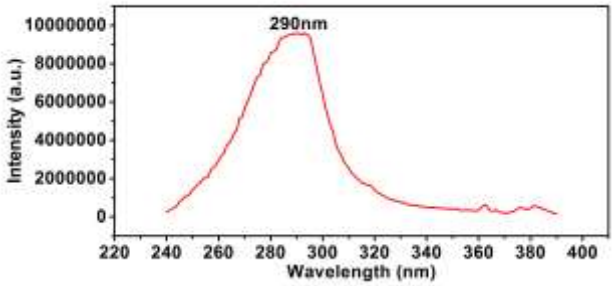

(a)

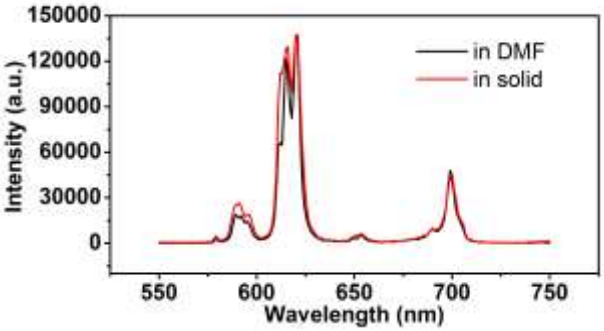

(b)

Fig. S9 The solid-state (a) excitation (monitored at 620 nm) and (b) emission (excited at 290 nm) spectra in DMF solution (black) or in solid state (red) of **1-pyr** at room temperature.

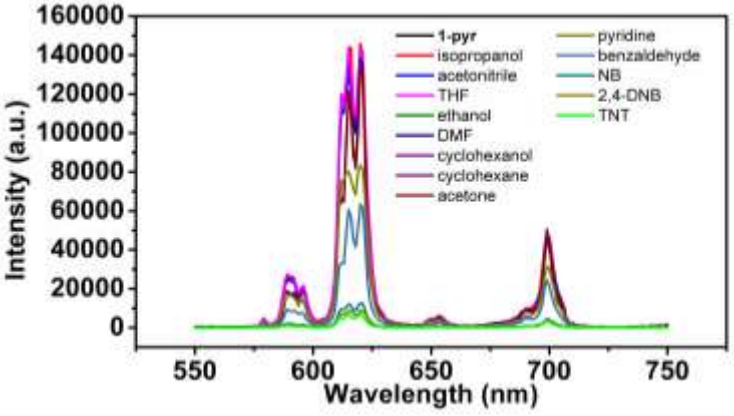

Fig. S10 Emission spectra of **1-pyr** in DMF emulsions with the addition of 5mM different solvents, monitored and excited at 620nm and 290nm, respectively.

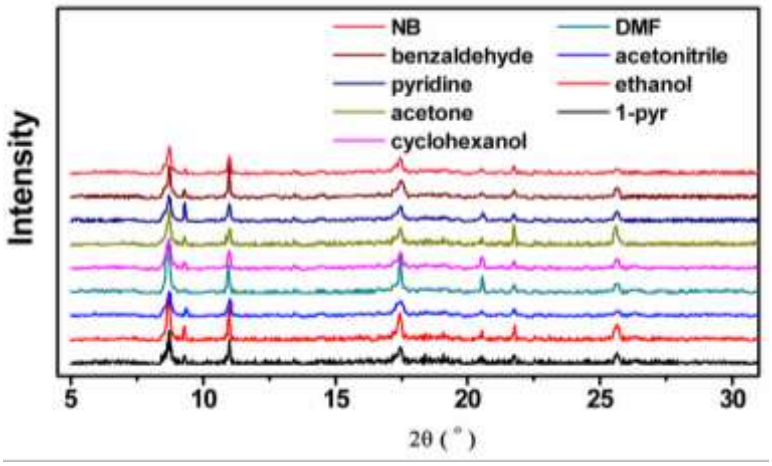

Fig. S11 Comparison of PXRD patterns of **1-pyr** dispersed in different solvents.

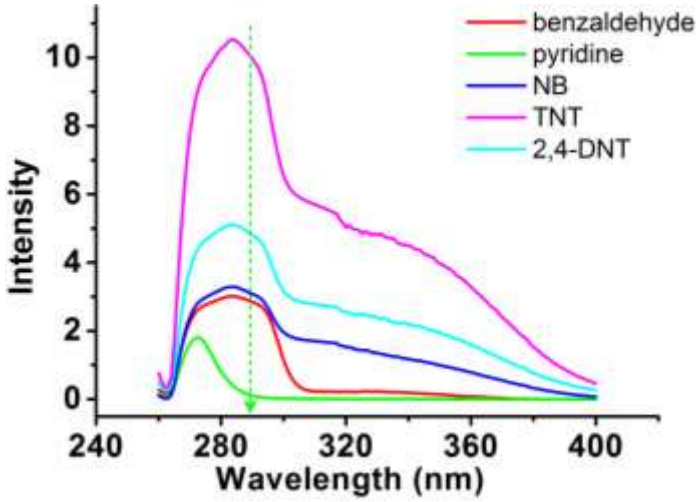

Fig. S12 UV-Vis absorbance spectra of 5mM aromatic compounds dissolved in DMF solution.

S1 G. M. Sheldrick, *Acta Crystallographica. A*, 2007, **64**, 112.
S2 A. Spek, *J. Appl. Crystallogr*., 2003, **36**, 7.
S3 B. Zheng, H. Liu, Z. Wang, X. Yu, P. Yi and J. Bai, *CrystEngComm*, 2013, **15**, 3517.
S4 D. Saha, Z. Bao, F. Jia and S. Deng, *Environ. Sci. Technol.* , 2010, **44**, 1820.
S5 B. Li, Z. Zhang, Y. Li, K. Yao, Y. Zhu, Z. Deng, F. Yang, X. Zhou, G. Li, H. Wu, N. Nijem, Y. J. Chabal, Z. Lai, Y. Han, Z. Shi, S. Feng and J. Li, *Angewandte Chemie-International Edition*, 2012, **51**, 1412.
S6 Y. Yan, M. Suyetin, E. Bichoutskaia, A. J. Blake, D. R. Allan, S. A. Barnett and M. Schröder, *Chemical Science*, 2013, **4**, 1731.
S7 S. R. Caskey, A. G. Wong-Foy and A. J. Matzger, *J. Am. Chem. Soc.* , 2008, **130**, 10870.
S8 X.-S. Wang, M. Chrzanowski, W.-Y. Gao, L. Wojtas, Y.-S. Chen, M. J. Zaworotko and S. Ma, *Chemical Science*, 2012, **3**, 2823.
S9 Y. Liu, J.-R. Li, W. M. Verdegaal, T.-F. Liu and H.-C. Zhou, *Chemistry - A European Journal*, 2013, **19**, 5637.
S10 B. Zheng, J. Bai, J. Duan, L. Wojtas and M. J. Zaworotko, *J. Am. Chem. Soc.* , 2011, **133**, 748.